

Successive Interference Cancellation for Optical Fiber Using Discrete Constellations

Alex Jäger, Gerhard Kramer

Institute for Communications Engineering, School of Computation, Information and Technology, Technical University of Munich, 80333, Munich, Germany, alex.jaeger@tum.de, gerhard.kramer@tum.de

Abstract Successive interference cancellation is used to detect discrete modulation symbols transmitted over a 1000 km fiber-optic link. A transmitter and receiver are presented that have linear complexity in the number of transmitted symbols and achieve the information rates of previous studies that use continuous modulations. ©2024 The Author(s)

Introduction

We investigate communication via wavelength-division multiplexing (WDM) through optical networks where receivers can access only their own WDM channel. Motivated by first-order regular perturbation^{[1],[2]}, the distortions caused by cross-phase modulation (XPM) are modeled as phase noise with correlations over many symbols^{[3],[4]}. Lower bounds on the end-to-end mutual information (MI) after joint detection and decoding (JDD) were developed in^{[5],[6]} by using particle filtering. However, it is not obvious how to combine such receiver algorithms with concrete coded modulations. For example, turbo detection and decoding^{[7]–[9]} is an option but requires dedicated code design and receiver iterations^[10]. Instead, a receiver that uses successive interference cancellation (SIC) allows using off-the-shelf codes^[11]; see also^{[12]–[14]}. Prior work studied receiver performance for continuous alphabet signaling. In this contribution, we investigate discrete modulation using probabilistically-shaped star quadrature-amplitude modulation (QAM).

System Model

Consider transmitting a vector x of n symbols sampled independently from a constellation \mathcal{X} . After pulse-shaping with a sinc-filter, the signal propagates over a channel described by the nonlinear Schrödinger equation (NLSE). The signal is disturbed by WDM signals co-propagating at different wavelengths, and the receiver can access only the wavelengths of interest through a bandpass filter. The receiver applies sampling, single-channel digital backpropagation (DBP), matched filtering using a sinc-filter and downsampling to symbol rate to obtain the received vector y .

The receiver approximates the channel from the input x to the output y using a correlated phase and additive noise (CPAN) model^[6]:

$$y_i \approx x_i e^{j\theta_i} + n_i \quad (1)$$

where the phase noise is modeled as a Gaussian process $\theta_i = \mu_\delta \theta_{i-1} + \sigma_\delta \delta_i$ where δ_i is sampled

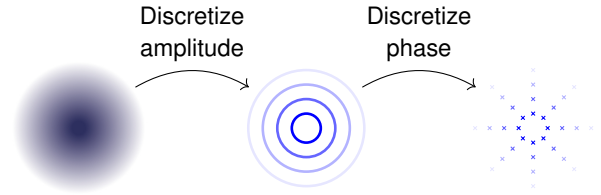


Fig. 1: Discretizing a CSCG density to obtain a shaped star QAM constellation. Brightness indicates a-priori probability.

independent of θ_{i-1} and x from a standard Gaussian distribution. The values μ_δ and σ_δ are chosen so the steady-state variance $\sigma_\theta^2 = \sigma_\delta^2 / (1 - \mu_\delta^2)$ has a desired value which can be found by training^[6]. The additive noise n_i is sampled from a circularly symmetric complex Gaussian (CSCG) distribution with variance σ_n^2 . We thus have the complex-alphabet surrogate channel model

$$q(y_i | x_i, \theta_i) = \frac{1}{\pi \sigma_n^2} \exp\left(-\frac{|y_i - x_i e^{j\theta_i}|^2}{\sigma_n^2}\right) \quad (2)$$

and the conditional probability density function (pdf)

$$p(\theta_i | \theta_{i-1}) = \mathcal{N}(\theta_i; \mu_\delta \theta_{i-1}, \sigma_\delta^2) \quad (3)$$

where $\mathcal{N}(x; \mu, \sigma^2)$ is a Gaussian pdf in x with mean μ and variance σ^2 .

Constellation Design

The receiver design in^[11] requires the conditional pdf $q(y_i | \theta_i) = \int p(x_i) q(y_i | x_i, \theta_i) dx_i$ to be constant in θ_i , which is the case for CSCG and unidistant Rayleigh ring (URR) distributions. The latter is a ring constellation obtained by discretizing a CSCG in amplitude.

To obtain a discrete constellation, we further discretize URR distributions in phase to obtain probabilistically-shaped star-QAM constellations, see Fig. 1. The absolute value r_i and phase γ_i of x_i are modulated independently and have probability mass functions (pmfs)

$$P(r_i) = \frac{r_i}{C} \exp\left(-\frac{r_i^2}{P_{\text{tx}}}\right), \quad P(\gamma_i) = \frac{1}{n_p} \quad (4)$$

where P_{tx} is the average transmit power, C is a normalization constant, and n_p is the cardinality of the

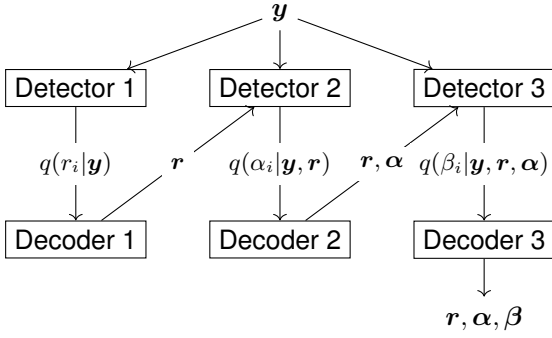


Fig. 2: SIC with two stages.

phase set $\left\{0, \frac{2\pi}{n_p}, 2\frac{2\pi}{n_p}, \dots, (n_p - 1)\frac{2\pi}{n_p}\right\}$. For these constellations, $q(y_i|\theta_i) = \sum_{x_i} P(x_i)q(y_i|x_i, \theta_i)$ is approximately constant in θ_i , and the approximation error increases in the distance of consecutive points with the same amplitude r_i , hence decreases in n_p .

Successive Interference Cancellation

For decoding, it is practical to have independent information for each data symbol x_i . For example, the separate detection and decoding (SDD) a-posteriori metric for x_i is $q(x_i|\mathbf{y})$. In contrast, the JDD a-posteriori metric $q(\mathbf{x}|\mathbf{y})$ has dependencies that give side information for each data symbol and provide improved achievable information rates (AIRs) compared to SDD. However, this metric is usually too complex for practical decoding.

We use SIC to provide practical a-posteriori metrics while keeping the loss in terms of AIR compared to JDD small. For two SIC-stages, the phase $\boldsymbol{\gamma} = [\gamma_1, \gamma_2, \dots]$ of the transmit vector is divided into vectors $\boldsymbol{\alpha}$ and $\boldsymbol{\beta}$ of length $n/2$ in the fashion $\boldsymbol{\gamma} = [\alpha_1, \beta_1, \alpha_2, \beta_2, \dots]$. The algorithm operates as follows; see Fig. 2.

1. Detect and decode the absolute value using SDD. Detector 1 passes a-posteriori information $q(r_i|\mathbf{y})$ to decoder 1. Decoding is error-free for long error-correcting codes and transmission rates below the AIR.
2. Decoder 1 passes \mathbf{r} to detector 2, which computes and passes a-posteriori information $q(\alpha_i|\mathbf{y}, \mathbf{r})$ to decoder 2.
3. Decoder 2 passes \mathbf{r} and $\boldsymbol{\alpha}$ on to detector 3 which computes and passes a-posteriori information $q(\beta_i|\mathbf{y}, \mathbf{r}, \boldsymbol{\alpha})$ to decoder 2.

Receiver Algorithm

For the absolute values, a memoryless detector $q(r_i|y_i)$ provides the same AIR as an SDD-detector $q(r_i|\mathbf{y})$ and a JDD-detector $q(\mathbf{r}|\mathbf{y})$ ^[11]. We find that $q(r_i|\mathbf{y})$ is proportional to

$$\sum_{\gamma_i} \int_{-\infty}^{\infty} P(r_i)P(\gamma_i)p(\theta_i)q(y_i|r_i, \gamma_i, \theta_i)d\theta_i. \quad (5)$$

Using (4) and

$$\sum_{\gamma_i} q(y_i|r_i, \gamma_i, \theta_i) \approx \int_{-\pi}^{\pi} q(y_i|r_i, \gamma'_i, \theta_i)d\gamma'_i \propto f_i(r_i) \quad (6)$$

with

$$f_i(r_i) = \exp\left(-\frac{r_i^2}{\sigma_n^2}\right) I_0\left(\frac{2|y_i|r_i}{\sigma_n^2}\right) \quad (7)$$

gives the mismatched a-posteriori

$$q(r_i|\mathbf{y}) = \frac{P(r_i)f_i(r_i)}{\sum_{\tilde{r}} P(\tilde{r})f_i(\tilde{r})} \quad (8)$$

where $I_0(\cdot)$ is the modified Bessel function of the first kind and zeroth order.

For the first stage of phase detection, a memoryless detector suffices^[11]. For odd i , $q(\gamma_i|\mathbf{y}, \mathbf{r})$ is proportional to

$$\int_{-\infty}^{\infty} P(r_i)P(\gamma_i)p(\theta_i)q(y_i|r_i, \gamma_i, \theta_i)d\theta_i. \quad (9)$$

The pdf $q(y_i|r_i, \gamma_i, \theta_i)$ is approximately proportional to the Gaussian pdf

$$\mathcal{N}\left(\theta_i; m(\angle y_i - \gamma_i), \frac{\sigma_n^2}{2|y_i|r_i}\right) \quad (10)$$

and using $p(\theta_i) = \mathcal{N}(\theta_i; 0, \sigma_\theta^2)$, we have

$$q(\gamma_i|\mathbf{y}, \mathbf{r}) = \frac{g_i(\gamma_i)}{\sum_{\tilde{\gamma}} g_i(\tilde{\gamma})} \quad (11)$$

$$g_i(\gamma_i) = \mathcal{N}\left(m(\angle y_i - \gamma_i); 0, \sigma_\theta^2 + \frac{\sigma_n^2}{2|y_i|r_i}\right) \quad (12)$$

where $m(x) = (x + \pi \bmod 2\pi) - \pi$ maps x to the interval $[-\pi, \pi)$.

For the second SIC-stage of phase detection, we use algorithm 1 in^[11] with inputs \mathbf{y} , \mathbf{r} and $\boldsymbol{\alpha}$. This algorithm uses approximate message passing so that $5n - 3$ messages, each containing a mean and variance, are passed along a factor graph to produce n outputs, each containing a mean and a variance. We collect the outputs in the vectors $\boldsymbol{\mu}$ and $\boldsymbol{\sigma}^2$, respectively. The corresponding a-posteriori metric for even i is now^[11]

$$q(\gamma_i|\mathbf{y}, \mathbf{r}, \boldsymbol{\alpha}) = \frac{h_i(\gamma_i)}{\sum_{\tilde{\gamma}} h_i(\tilde{\gamma})} \quad (13)$$

$$h_i(\gamma_i) = \mathcal{N}\left(m(\angle y_i - \gamma_i - \mu_i); 0, \sigma_i^2 + \frac{\sigma_n^2}{2|y_i|r_i}\right). \quad (14)$$

For more SIC-stages, the algorithm described for the second stage is applied repeatedly.

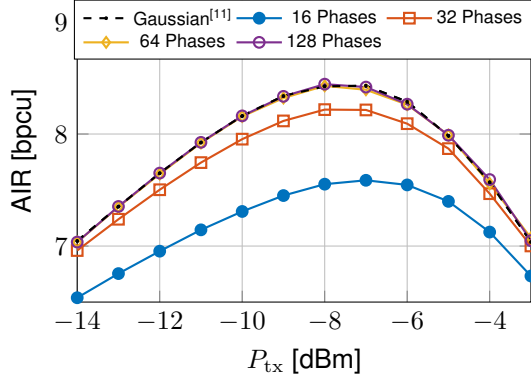


Fig. 3: AIR of star-QAM with 32 rings and varying n_p compared to that of a CSCG using two SIC-stages.

Simulation Results

We use the same simulation setup as in^{[5],[6],[11]} with a 1000 km link and ideal distributed Raman amplification. We use 24 sequences of 8192 symbols each to obtain μ_δ , σ_δ^2 , σ_θ^2 and σ_n^2 , and 120 sequences of 8192 symbols each for testing.

Fig. 3 shows the AIRs of star-QAM with 32 rings and varying cardinality of the phase constellation n_p using 2 SIC-stages. We also plot the AIRs of CSCG modulation. The AIR increases with n_p up to $n_p = 64$ where the AIR of CSCG is met and saturates. Since the star-QAM constellations resemble CSCGs for a large number of rings and large n_p , this result is intuitive. However, it is unclear if the loss for small n_p is due to poor constellation design or approximation errors arising from assuming $q(y_i|\theta_i)$ is constant in θ_i . We remark that, since the AIR of the phase channel is below 5 bpcu^[11], it could be supported by 32 phases.

To investigate the issue, Fig. 4 shows that star-QAM constellations with 32 rings and 32 phases experience a noticeable loss of AIR compared to CSCG modulation even for memoryless additive white Gaussian noise (AWGN)-channels. We thus expect that the loss in Fig. 3 is due to the small phase constellation cardinality rather than an approximation error.

Fig. 5 plots the average AIRs of star-QAM with 32 rings and 128 phases. We compare performance to those of a mismatched receiver based on memoryless AWGN surrogate channels, a receiver using JDD and particle filtering^[6], and an upper bound on capacity^[15]. The curve for 2 SIC-stages is already closer to the JDD curve than to the memoryless AWGN curve. This is because the AWGN curve does not account for the phase noise process and is smaller than the first-stage AIR, and the second-stage AIR is already close to the JDD AIR. Observe that the average AIR increases with the number of SIC-stages until it saturates near the AIR of JDD at 16 or more SIC-stages. The curves suggest that 2-4 SIC-stages might suffice for practical implementations.

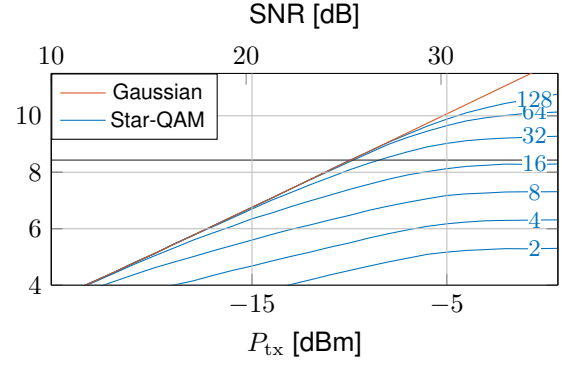


Fig. 4: AIR of memoryless AWGN channels with noise variance σ_n^2 using 32 rings.

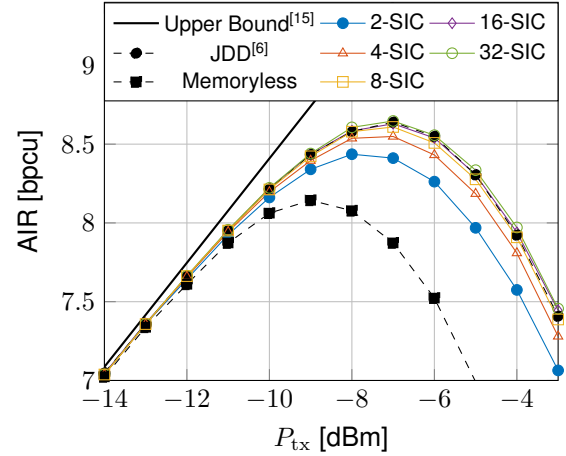


Fig. 5: AIR of star-QAM with 32 rings, 128 phases, and a varying number of SIC-stages.

Outlook

The proposed transmitter and receiver show competitive performance in mitigating phase noise with long correlations, similar to a genie-aided receiver that can fully compensate for phase noise^[11]. To further increase the AIR, one might focus on the inter-symbol interference (ISI) caused by XPM.

For future work, the receiver could be generalized to incorporate single-channel DBP. For this purpose, one must pay attention to nonlinear phase noise and strong additive noise terms caused by self-phase modulation (SPM)^[3]. Note that SPM can create additive noise through strong two-pulse collisions, whereas XPM creates only phase noise through such collisions^[4].

Conclusion

We extended the SIC-receiver studied in^[11] to discrete modulation alphabets, in particular probabilistically-shaped star-QAM constellations. We recovered the AIRs computed in^[11] using SIC and CSCG, and the AIRs in^[6] using JDD and particle filtering, for a 1000 km transmission link. We found that 32 rings and 128 phases suffice when using 16 SIC-stages. Also, 2-4 SIC-stages offer a good trade-off between performance and computational cost and might hence be interesting for practical implementations.

Acknowledgements

The authors acknowledge the financial support by the Federal Ministry of Education and Research of Germany in the programme of “Souverän. Digital. Vernetzt.” Joint project 6G-life, project identification number: 16KISK002.

References

- [1] A. Vannucci, P. Serena, and A. Bononi, “The rp method: A new tool for the iterative solution of the nonlinear schrodinger equation”, *Journal of Lightwave Technology*, vol. 20, no. 7, pp. 1102–1112, 2002. DOI: 10.1109/JLT.2002.800376.
- [2] A. Mecozzi and R.-J. Essiambre, “Nonlinear shannon limit in pseudolinear coherent systems”, *Journal of Lightwave Technology*, vol. 30, no. 12, pp. 2011–2024, 2012. DOI: 10.1109/JLT.2012.2190582.
- [3] R. Dar, M. Feder, A. Mecozzi, and M. Shtaf, “Properties of nonlinear noise in long, dispersion-uncompensated fiber links”, *Optics Express*, vol. 21, no. 22, pp. 25 685–25 699, 2013. DOI: 10.1364/OE.21.025685.
- [4] R. Dar, M. Feder, A. Mecozzi, and M. Shtaf, “Pulse collision picture of inter-channel nonlinear interference in fiber-optic communications”, *Journal of Lightwave Technology*, vol. 34, no. 2, pp. 593–607, 2016. DOI: 10.1109/JLT.2015.2428283.
- [5] M. Secondini, E. Agrell, E. Forestieri, D. Marsella, and M. R. Camara, “Nonlinearity mitigation in wdm systems: Models, strategies, and achievable rates”, *Journal of Lightwave Technology*, vol. 37, no. 10, pp. 2270–2283, 2019. DOI: 10.1109/JLT.2019.2901908.
- [6] F. J. García-Gómez and G. Kramer, “Mismatched models to lower bound the capacity of optical fiber channels”, *Journal of Lightwave Technology*, vol. 38, no. 24, pp. 6779–6787, 2020. DOI: 10.1109/JLT.2020.3021277.
- [7] C. Douillard, M. Jézéquel, C. Berrou, *et al.*, “Iterative correction of intersymbol interference: Turbo-equalization”, *European Transactions Telecommunications*, vol. 6, no. 5, pp. 507–511, 1995. DOI: 10.1002/ett.4460060506.
- [8] G. Colavolpe, A. Barbieri, and G. Caire, “Algorithms for iterative decoding in the presence of strong phase noise”, *IEEE Journal on Selected Areas in Communications*, vol. 23, no. 9, pp. 1748–1757, 2005. DOI: 10.1109/JSAC.2005.853813.
- [9] M. P. Yankov, T. Fehenberger, L. Barletta, and N. Hanik, “Low-complexity tracking of laser and nonlinear phase noise in wdm optical fiber systems”, *Journal of Lightwave Technology*, vol. 33, no. 23, pp. 4975–4984, 2015. DOI: 10.1109/JLT.2015.2493202.
- [10] S. ten Brink, G. Kramer, and A. Ashikhmin, “Design of low-density parity-check codes for modulation and detection”, *IEEE Transactions on Communications*, vol. 52, no. 4, pp. 670–678, 2004. DOI: 10.1109/TCOMM.2004.826370.
- [11] A. Jäger and G. Kramer, “Information rates of successive interference cancellation for optical fiber”, *IEEE Journal on Selected Areas in Communications*, submitted, 2024. arXiv: 2403.15240.
- [12] U. Wachsmann, R. Fischer, and J. Huber, “Multilevel codes: Theoretical concepts and practical design rules”, *IEEE Transactions on Information Theory*, vol. 45, no. 5, pp. 1361–1391, 1999. DOI: 10.1109/18.771140.
- [13] H. Pfister, J. Soriaga, and P. Siegel, “On the achievable information rates of finite state ISI channels”, in *GLOBECOM’01. IEEE Global Telecommunications Conference*, vol. 5, 2001, pp. 2992–2996. DOI: 10.1109/GLOCOM.2001.965976.
- [14] D. Plabst, T. Prinz, F. Diedolo, *et al.*, “Neural network equalizers and successive interference cancellation for bandlimited channels with a nonlinearity”, *IEEE Transactions on Communications*, submitted, 2024. arXiv: 2401.09217.
- [15] G. Kramer, M. I. Yousefi, and F. R. Kschischang, “Upper bound on the capacity of a cascade of nonlinear and noisy channels”, in *2015 IEEE Information Theory Workshop (ITW)*, 2015, pp. 1–4. DOI: 10.1109/ITW.2015.7133167.